Differential metabolic composition of the uterine fluid from fertile and subfertile hens after artificial insemination

Cindy Riou, Luiz Cordeiro, Lydie Nadal-Desbarats, Nadine Gérard

Differential metabolic composition of the uterine fluid from fertile and subfertile hens after artificial insemination

Cindy Riou [1,2], Luiz Cordeiro [1,3], Lydie Nadal-Desbarats[4], Nadine Gérard [1,5]

[1] CNRS, IFCE, INRAE, Université de Tours, PRC, 37380, Nouzilly, France

[2] ALLICE, Station de Phénotypage, Lieu-Dit Le Perroi, 37380 Nouzilly, France

[3] Federal University of Semi Arid Region, Mossoro, 59625-900, Rio Grande do Norte, Brazil

[4] Département de biochimie, UMR Inserm U 1253, Université de Tours, 10 Boulevard Tonnellé 37032, Tours, France

[5] Corresponding author. Email: nadine.gerard@inrae.fr

Abstract

Avian uterine fluid (UF) has been demonstrated to prolong sperm survival, to maintain the fertility potential of the fowl sperm, and to impact the filling rate of sperm storage tubules (SST) from the utero-vaginal junction (UVJ). The purpose of this study was to identify UF metabolites related to long-term sperm storage.

Two genetic lines of hens exhibiting long (F+) or short (F-) sperm storage ability were used. Metabolites present in the UF either before or after insemination were identified and quantified using high resolution ^{1}H-NMR. The effect of the presence of sperm was investigated 24 hours, 1 week, 2 weeks and 3 weeks after a single artificial insemination.

Thirteen metabolites were identified as discriminating between the UF collected before insemination from the two lines of hens. Among them, formate, organic acids (succinate, fumarate, lactate), dimethylamine and arabinose were significantly more abundant in F+ UF, whereas myo-inositol was significantly more abundant in F- UF ($p<0.05$). Pathway and metabolite set enrichment analyses revealed that preponderant metabolic pathways were over

representated in the F+ UF and involved pyruvate metabolism, citrate cycle and steroid biosynthesis ($p<0.05$). No metabolite was identified as discriminating in F+ UF, when compared before and after insemination. In contrast in the F- line of hens, 11 metabolites discriminated the UF collected before and after insemination. Actually, we observed that dimethylamine was significantly reduced, while fumarate and myo-inositol metabolites were significantly increased. Moreover, Warburg effect pathway involving glucose to lactate metabolism, was significantly enriched in F- after insemination.

Our results indicate that in the hen, the metabolic composition of UF is related to the genetic traits F+/F-, and is differentially modified after insemination in both lines. It could be related to sperm storage. These lead us to conclude that: 1) the UF biochemical composition is associated with the sperm survival ability in SST, 2) is regulated by the presence of sperm, and 3) this regulation is related to the sperm survival ability in SST.

Key words: sperm storage, metabolomic, chicken, uterine fluid, fertility, ^{1}H-NMR

Introduction

The avian female reproductive tract is divided in 5 segments including infundibulum, magnum, white isthmus, uterus and vagina, which are associated with the egg components. After ovulation, the oocyte (yolk) enters the infundibulum where fertilization can take place. It then goes through magnum and isthmus consecutively for the deposition of the vitelline membrane outer layer, egg white (0.5 to 3.5 hours post ovulation) and eggshell membranes (3.5 to 5 hours post ovulation), respectively. Eggshell calcification occurs in the uterus within an 18 hours period. During this period, the egg mass in the uterus compresses the uterovaginal (UVJ) folds that are positioned towards the uterus (Bakst & Akuffo, 2009). Lastly, the egg passes through the vagina and is laid 24 hours after ovulation.

It is well known that female birds are able to produce fertilized eggs for several days, even weeks or months following a single mating (i.e. quail 11 days, hen 3 weeks, turkey 3 months). Actually, after mating sperm ascent the vagina and is stored in specialized structures named uterovaginal sperm storage tubules (UVJ-SST). UVJ-SST have been described in several avian species, and it is well known that they allow the preservation of sperm for long periods (Birkhead & Moller, 1993; Bakst et al., 1994, Brillard, 1993). Sperm cells are gradually released from UVJ-SST to transit to the infundibulum, the fertilization site. Ahammad et al. (2013) demonstrated that the filling of uterovaginal SST is more efficient when insemination is performed at the initialization of eggshell mineralization (i.e. 5-6 hours after ovulation) than the calcifying phase (Ahammad et al., 2013).

The mechanisms by which sperm survive and maintain their fertilizing abilities is not clear, and only little is known about the biochemical and/or cellular interactions involved between sperm, uterine fluid (UF) and oviductal cells. Local secretions (Froman, 2003; Bakst & Akuffo, 2007; Riou et al., 2017; Riou et al., 2019, 2020) as well as specific interactions between sperm and SST epithelium cells (Tingari & Lake, 1973; Das et al., 2008; Bakst & Bauchan, 2015) may play crucial roles to preserve sperm. Of note that during both storage in UVJ-SST and ascent from the vagina to the infundibulum, sperm are exposed to the UF. It has been shown that the UF collected during the initialization of eggshell mineralization promotes the maintenance of sperm motility and viability in vitro (Brillard et al., 1987; Ahammad et al., 2013). The same authors demonstrated that hens inseminated with sperm exposed to "initialization phase" UF exhibit a longer period of fertile egg production compared to hens inseminated with sperm exposed to "calcifying phase" UF (Brillard et al., 1987; Ahammad et

al., 2013). This suggests that UF composition varies throughout the day, in relation to the stage of egg formation, and that some UF components are able to regulate sperm functions such as sperm storage ability and duration. Consequently, we can hypothesize that some UF components or metabolites are essential for sperm functions, such as sperm storage efficiency in birds.

UF represents the aqueous environment in which sperm are exposed during storage and transit through the female tract. Its composition has been widely investigated in regards to the egg formation (Gautron et al., 2019). Daily ovulation cycle gives rhythm to the UF protein composition, which is responsible of sequential eggshell deposition (Sun et al., 2013; Marie et al., 2015). Recently, it has been shown that sperm arrival in SST induces a rapid modification of UF protein composition, and of transcriptomic patterns of uterine tissue (Long et al., 2003; Atikuzzaman et al., 2015; Riou et al., 2019). These observations suggest that sperm regulate UF composition.

A major physiological role of UF metabolites has been described in relation to the sperm storage process. In quail SST, sperm are stored immobile under low oxygen and high lactic acid concentrations (Matsuzaki et al., 2015) that induces flagellar quiescence. Therefore, it is admitted that the long-term sperm storage in avian species may involve specific metabolic conditions, which enable sperm to survive. We could suggest that these specific metabolic conditions may originate at least in part from UF, and could extend the sperm survival time.

In this study, we hypothesized that UF collected during the initiation of eggshell mineralization contains specific metabolites which promote the long-term sperm storage. Therefore, our study aimed to characterize metabolites that are present in UF from fertile (F+) and subfertile (F-) hens during 3 weeks after artificial insemination. This two lines of hens exhibit a long (F+) or short (F-) duration of fertile period, as a consequence of a good or poor ability for a long-term sperm storage in uterovaginal SST, respectively (Brillard et al., 1998).

We expected to reveal specific metabolite patterns associated to the long-term sperm storage process. We clearly demonstrated that avian UF contains metabolites which may play key role in the long-term sperm storage process.

Materials and methods

Birds

Sexually mature hens issued from two genetic lines previously selected for their ability to produce normal (F+) or low (F-) numbers of hatched chicks, and to preserve sperm in their SST for a long (F+) or short (F-) period of time, were used in this study. These two lines were different in the duration of their fertile period, the F- line expressing a shorter time potential to lay fertile eggs than the F+ line (Beaumont et al., 1992). Breeding procedures and handling protocols were carried out according to the European Community Council Directives regarding the practice for care and use of animals and of the recommendations of the French Ministry of Agriculture on Animal Experimentation under the supervision of an authorized scientist (Authorization # 37035). Farm facilities (Institut National de la Recherche Agronomique, UE-PEAT, 1295) are recognized as officially authorized to rear and euthanize birds (27-175-1). At 47 wks of age, hens were placed in individual cages equipped with automatic devices to record the time of oviposition. They were kept under a 16L: 8D photoperiod, and fed a layer mash *ad libitum*. The protocol of bird management and collection was approved by the local ethical comity (Comité d'éthique de Val de Loire n°19) and the French ministry under agreement number # 443.

Evaluation of fertility performance

The duration of the fertile period within each line was expressed using two definitions: effective duration (De), the number of days after artificial insemination (AI) during which a hen lays 100 % fertile eggs; and maximum duration (Dm), the number of days after AI until the hen lays its last fertile egg. At 50 wks of age, hens were inseminated on two consecutive days (Day 0 and Day 1) with 200 x 10^6 sperm from mixed ejaculates collected from 6 broiler breeder males on both days. The eggs were identified individually and recorded daily from Day 2 to Day 22. They were stored at room temperature for a maximum of 7 days and incubated for 7 days . The percentage of fertile eggs was determined by candling at the end of the incubation period. Eggs primarily classified as infertile were broken up for macroscopic examination of the germinal disc to determine the presence/absence of dead blastodiscs. Comparisons for De, Dm, and fertility, laying and embryo mortality rates between the two lines were computed using a Mann-Whitney test ($P < 0.05$). Sixteen hens (7 F+ and 9 F- hens) were then selected from the 60 hens according to the evaluation of fertility performance.

Uterine fluid (UF) collection

UF collection for hen's that were not subjected to insemination was planned 10h after the previous oviposition and after confirming the presence of an egg in utero. Egg expulsion was carried out by intravenous injection of prostaglandin F2α at 50µg/hen. UF was collected immediately after egg expulsion, into a plastic tube placed at the entrance of the everted vagina before insemination (virginized hens) and 24 hours, 1 week, 2 weeks and 3 weeks after artificial insemination (Gautron et al., 1997). Aliquot of fluid was diluted with PBS (1v:1v) in order to perform ^{1}H-NMR analysis. All aliquots were rapidly frozen in liquid nitrogen to limit any spontaneous precipitation of calcium carbonate and proteins, and stored at -20°C (Hincke et al., 1999).

^{1}H-NMR sample preparation

UF were prepared for the high-resolution proton nuclear magnetic resonance (^{1}H NMR) analyses by cold methanol precipitation of lipids and proteins. The unfrozen samples were centrifuged at 15,000 g for 10 min at 4 °C. After this, 450 µL of the supernatants were mixed with 1 mL of methanol and cooled at −20 °C for 20 min. The mixtures were then centrifuged as previously described, and 1,150 µL of the supernatants were collected in glass tubes for further solvent evaporation in a SpeedVac (ThermoScientific, Villebon sur Yvette, France) at room temperature and conserved at −20 °C.

^{1}H-NMR spectroscopy measurements

Before NMR analysis, the extracted UF samples were reconstituted in 220 µL pH 7.4 potassium phosphate buffer in 99% deuterium oxide (D_2O) with 0.128 mM trimethylsilylpropionic acid (TSP) as an internal reference. After centrifugation at 4,000 g for 15 min at 4 °C to remove any insoluble components, the supernatant was transferred to conventional 3 mm NMR tubes, for NMR analysis. High-resolution ^{1}H NMR spectra from the UF were acquired on a DRX-600 Avance III HD spectrometer (Bruker SADIS, Wissembourg, France), operating at 600.13 MHz, with a TCI cryoprobe. NMR measurements were performed at 298 K. Standard ^{1}H NMR spectra were acquired using a "cpmgpr-1d" pulse sequence with a relaxation delay of 25 s, an echo time of 80 ms (64 scans), and a time domain of 32,768 points. Water suppression was achieved by presaturation during the relaxation delay. Spectra were processed using Topspin version 3.2 software (Bruker Daltonik, Karlsruhe, Germany). The free induction decays (FIDs) were zero-

filled to 65,536 data points, which provided sufficient data points for each resonance, and a line-broadening factor of 0.2 Hz was applied before Fourier transformation.

NMR Spectra Post-processing

After manual correction of the phase distortion and baseline on all spectra, the ^{1}H NMR spectra were imported into AMIX software (version 3.8.4; Bruker). The bin area method was used to segment the spectra between 0.6 and 9 ppm using the intelligent variable size bucketing tool. The spectral region containing water was excluded and a total of 64, 160, and 191 buckets were defined manually for serum, ileal content and caecal content spectra, respectively. Those bin areas corresponding to one or several metabolites were normalised by dividing each integrated segment by the total area of the spectrum on the 3 data sets.

Spectral Assignment

The ^{1}H NMR spectra, referenced to the internal TSP chemical shift reference, were assigned using spectra from our in-house database and online databases, including LMDB (http://www.lmdb.ca) or the Chenomx NMR Suite 7.7 evaluation edition (Chenomx Inc, Edmonton, Canada).

Statistical analysis

Multivariate analysis was performed using SIMCA 13 software (version 13.0, Umetrics, Umeå, Sweden) on the **two datasets, i.e. F+ H-NMR and F- H-NMR**. All data were scaled to unit variance to maximize the separation between F+ and F- lines of hens. OPLS-DA is a method of supervised classification that predicts the categorical factor (defined here by the two chicken lines) by explanatory quantitative variables (defined here by the spectral bins or metabolites). Variation in the spectral bins data X is divided into one predictive component, containing variations correlated with the class identifier Y (F+ or F- line) and single or multiple orthogonal components containing variations orthogonal to the predictive component that do not contribute to discrimination between the defined groups. By separating predictive and non-predictive components, OPLS-DA is more adapted than PLS-DA to predict biological variables that usually contain multiple sources of variation that are potentially not correlated with the predicted variable. The overall quality of the model for the **two datasets** analyzed was judged by cumulative R2Y, defined as the proportion of variance in Y explained by the predictive component of the model and cumulative Q2, the class prediction ability of the model obtained

by the cross-validation default method (7 fold cross-validation) of SIMCA 13 Solftware: the higher R2Y (cum) and Q2 (cum) the better the separation between the lines. Cross-validation analysis of variance (CV-ANOVA) was applied to evaluate further the significance of the findings. To improve screening, the minimum of features (spectral bins) needed for optimal classification of the **two OPLS-DA models** (**F+ H-NMR and F- H-NMR**) was determined by iteratively excluding from the models the variables with low regression coefficients and high standard deviations combined with low VIP (Variable Importance in Projection) until improvement of the predictive component assessed by the maximization of Q2 (cum) and R2Y (cum) was achieved. Metabolites included in the model with a VIP > 1 were considered as important. The variable contribution plot also allowed evaluation of the contribution of each predictor in the model.

To identify the most relevant metabolites across the **two datasets**, an alternative model was fitted by multiblock OPLS-DA applied to the spectral bins previously identified by OPLS-DA of **F+ H-NMR and F- H-NMR,** and structured in the two blocks. In practice, a different block was assigned to the variables of each dataset and each block was scaled to avoid the domination of one block over the overs. Thereafter, OPLS-DA was performed on the three blocks iteratively, excluding the least relevant variables from the model as described above. The results from the multiblock model were computed with the results from the **two models** performed on each dataset separately.

T-test on the metabolite quantities. Following the OPLS-DA analyses, the equality of means between the two chicken lines for each discriminant metabolite was tested using univariate statistical analysis, computed with Metaboanalyst, a freely available web-based metabolomics analysis suite (MetaboAnalyst 4.0, http://www.metaboanalyst.ca/), consisted of non-parametric t-test (equal variances) at the 95% confidence level.

Pathway impact analysis

To identify the most significant impact of affected metabolic pathways, the OPLS-DA discriminating metabolites were analyzed using MetaboAnalyst 4.0 software. MetaboAnalyst software derives its predictive ability from the KEGG metabolic pathways database (last updated on October 2019), which includes the *Gallus gallus* library used in this study. The software incorporates several specific algorithms to identify the most significant pathway impact, such as the pathway enrichment analysis (global test), the pathway topology analysis

(global test) as well as the log fold change of the differential metabolites. A cutoff was chosen at a raw P-value of 1.0 to retain the most significantly pathway impact.

Metabolites set enrichment analysis

A Metabolite Set Enrichment Analysis (MSEA) was performed using the OPLS-DA discriminating metabolites to identify the biologically meaningful groups of metabolites in terms of pathway, disease and localization. MSEA derived from the gene set enrichment analysis (GSEA) ontology method. MSEA only supports human metabolic data. The metabolite enrichment analysis of each set of metabolites was performed using over-representation analysis (ORA) with the "Pathway-associated metabolite sets (SMPDB)" library containing 99 metabolite sets based on normal human metabolic pathways. The ORA was implemented using the hypergeometric test to evaluate whether a particular metabolite set was more highly representated than expected by chance within the given compound list. A cutoff was chosen at a raw P-value of 1.0 to retain the most significantly enriched metabolic pathways.

Results

Bird fertility traits

Two groups of hens from each genetic line were constituted, F+ (n=7) and F- (n=9). As illustrated in Figure 1 and Table 1, these lines differ mainly in sperm storage ability, i.e. their maximum duration of fertility (Dm). The efficient (De) and maximum (Dm) duration of fertility in the fertile F+ hens were ± and ± (days) respectively, nearly times and times higher than in the subfertile F- hens (± and ± days respectively). The fertility rates were 73.2 ± and 28.4± % for the two groups on the duration of 3 weeks, respectively (Figure 1). Thus, throughout this manuscript F- and F+ hens are referred to as subfertile and fertile hens. The laying rate and embryo mortality were not significantly different between the two genetic lines (not shown).

1H NMR Spectroscopic profiles

The annotated representative ^{1}H NMR spectrum of the oviductal fluid content extract sampled before insemination is shown in Figure 2. The experimental and spectral data were deposited under the accession number MTBLS0000 in the MetaboLights repository hosted by the EMBL-EBI (http://www.ebi.ac.uk/metabolights/MTBLS00000)

As presented in Figure 3A, the avian UF is mainly composed with organic acids (50%), which include formic acid, succinic acid, fumaric acid, lactic acid, and many others, as well as

derivates such as amino acids, peptides and analogues (creatinine, L-alanine). In second place, with 33% of metabolites, is the organic oxygen compounds super class, which includes several carbohydrates and carbohydrates conjugates. Among them, alpha -D-glucose which is the main metabolite of the avian UF (Figure 3B), arabinose, mannose, and glucuronic acid. Alcohol and polyols sub class is represented by myo-inositol and polypropylene glycol. Of note that myo-inositol is the second UF metabolite in terms of concentration (Figure 3B). Organic nitrogen compounds (i.e. amines, amides, nitrosamines, alkyl nitrates, and peroxyacyl nitrates) take 3rd place (6%) and are represented in the avian UF by dimethylamine, which ranks 11th in terms of concentration of UF metabolites (Figure 3B).

Multivariate Analysis of ^{1}H-NMR Spectral Data

OPLS-DA was carried out on the ^{1}H-NMR spectral data for (1) the comparison of F+ with F- UF at each time after insemination (genetic effect) and (2) the comparison in both genetic lines of UF collected before insemination (virginized hens) with UF collected at 24 hours or 1 week or 2 weeks or 3 weeks after insemination (insemination effect).

Genetic effect: The 4 models characteristic for the genetic effect are presented Figure 4A. The first model that compares virginized F+ and F- ^{1}H-NMR spectral data resulted in 1 predictive and 1 orthogonal component (1p + 1o) with the predictive ability *Q2*(cum) = 0.44 and the overall proportion of the variation in Y explained by the model *R2Y(cum)* = 0.69. The 2 genetic lines of hens are well separated, particularly by formic acid and succinic acid concentrations. This is illustrated by the score plot (Figure 4B) and comparisons of formic and succinic acid concentrations that were significantly different between the 2 lines (Figure 4C, $p < 0.05$). The 3 other models also resulted in one predictive and one orthogonal component (1p + 1o) with a specific predictive ability *Q2*(cum) and a specific overall proportion of the variation in Y explained by the model *R2Y(cum)*, as presented Figure 4A. The quality of prediction of the model *Q2*(cum) was high for all ^{1}H-NMR analysis. Of note that no model was found for the comparison of ^{1}1H-NMR spectral data obtained from F+ and F- UF collected 1 week after AI (Fig 4A).

The corresponding contribution plots generated by SIMCA software were used to identify the metabolites allowing chicken line discrimination with Metaboanalyst 4.0 software. The discriminating metabolites of UF determined by OPLS-DA, their respective VIP reflecting the importance of variables in the OPLS-DA models, F+ /F- fold-change, and their individual t-test *P*-values are listed in Table 2. The most discriminant metabolites that were significantly

different between the two genetic line and characterized by a high VIP value (VIP > 1.2) or metabolites with a high fold change value (FC >2) is presented in Figure 5.

Insemination effect. No significant model was found for the comparisons of F+ ^{1}H-NMR spectral data after insemination. In contrast, F- hens displayed significant differences for all comparisons. The 4 models comparing ^{1}H-NMR spectral data resulted in 1 predictive and 1 orthogonal component (1p + 1o) with predictive ability and overall proportion of the variation in Y, which values are presented in Figure 6A. The quality of prediction of the model (*Q2*(cum)) was high for both ^{1}H-NMR analysis. The corresponding contribution plots generated by SIMCA software were used to identify the metabolites allowing insemination effect discrimination with Metaboanalyst software. The discriminating metabolites of the uterine fluid determined by OPLS-DA, their respective VIP value, "after insemination (24 hours or 1 week or 2 weeks or 3 weeks) /virginized" fold-change, and their individual p-values are listed in Table 3. The most discriminant metabolites that were significantly different between each condition and characterized by high VIP value (VIP > 1.2) are presented in Figure 6B.

Pathway Impact and Metabolite Set Enrichment Analysis

Genetic effect. To identify the most significant impact of metabolic pathways involved in the genetic line effect, the discriminating metabolites (shown in Table 2) were analyzed using MetaboAnalyst 4.0 software. As shown in Figure 7A, two pathways that are pyruvate metabolism and citrate cycle (TCA cycle) were the most preponderant in F+ and F- UF ($p<0.05$). Pyruvate metabolism pathway involves several metabolites as lactacte, pyruvate and fumarate, which have been observed more abundant in F+ than in F- UF at all time, except at 2 weeks after insemination where fumarate was preponderant in F- UF ($p<0.05$). Citrate cycle pathway involved succinate, citrate, pyruvate and fumarate, which were preponderant in F+ UF comparing to F- ($p<0.05$).

Moreover, a Metabolite Set Enrichment Analysis (MSEA) was performed using all the discriminating metabolites (shown in Table 2) to identify the biologically meaningful groups of metabolites in terms of pathway, disease and localization, that are significantly enriched in the two lines of hens. MSEA only supports human metabolic data. Using the pathway associated metabolites sets (SMPDB) library which contains 99 metabolites sets, our analysis indicated that the most representative metabolic pathways were more abundant in the F+ line and involved pterine and steroid biosynthesis, folate metabolism, androgen, estrogen and androstenedione metabolism, tryptophan metabolism, arginine and proline metabolism and

mitochondrial electron transport chain ($p<0.05$) as illustrated in Figure 7B. Of note that formate is involved in androstenedione and tryptophan metabolism, L-alanine involved in tryptophan metabolism, and succinate and fumarate are involved in mitochondrial electron transport chain, all of them being discriminating metabolites between the two lines of hens.

Insemination effect. Pathway analysis on the discriminating metabolites after insemination in F- UF (shown in Table 3) revealed that three high impact-pathways that are starch and sucrose metabolism, ascorbate and aldarate metabolism and pentose and glucoronate interconversions that were preponderant after insemination (ns) (Figure 7A). These include myo-inositol and UDP-glucuronate which were observed more abundant at each time after insemination, and arabinose which was reduced after insemination ($p<0.05$, Table 3).

MSEA that concerns the insemination effect is illustrated in Figure 7B. It revealed that the 10 most representative metabolic pathways after insemination in F- line involved several amino acids metabolism, purine metabolism, citric acid and urea cycles, mitochondrial electron transport chain and Warburg effect ($p<0.05$) (Figure 7B). Of note that fumarate is involved in mitochondrial electron transport chain and Warburg effect, and that glucose and lactate are involved in Warburg effect. However, we have already observed that fumarate, lactate and glucose metabolites all significantly increased after insemination.

Discussion

We described in our study the metabolomic composition of the UF and analyzed it for three weeks after insemination in two divergent lines of hens that exhibit a long- or short-term sperm storage ability. We demonstrated that UF metabolomic composition is significantly different between the F+ and F- hens (genetic line effect). Despite no significant difference were found for F+ hens, UF metabolomics composition was affected after insemination in F- hens (insemination effect).

Metabolomic composition of the uterine fluid

Uterine fluid collected from F+ and F- hens was mainly constituted of glucose. It has been shown that UF glucose content varies during the process of egg formation (Brillard et al., 1987; Ahammad et al., 2013). Its presence in sperm extenders has been shown to supply energy to the sperm (van Tienhoven, 1960). In our study, we also identified UDP-glucuronate in the uterine fluid. This metabolite derives from glucose and participates to the constitution of proteoglycans and glycosaminoglycans, which composed the eggshell. Uterine fluid contained others

carbohydrates like mannose and arabinose, as well as low molecular weight metabolites including organic cyclohexanol (myo-inositol), creatinine, amino acid (alanine), organic secondary amine (dimethylamine) and several organic acids (lactate, citrate, acetate, formate, glucoronate, pyruvate, succinate, fumarate).

Genetic effect

In our analysis of the genetic effect, no significant SIMCA-models were found when we compared the UF metabolomic composition between the two lines of hens at one week after insemination. Interestingly at 10 days after insemination, it has been previously shown that females F+ inseminated with F+ semen can store more sperm in their SSTs than F- inseminated with F- semen (Brillard et al., 1998). This previous study also demonstrated that at three days after insemination, the number of stored sperm in SSTs is similar in both lines. In the interval between 3-10 days after insemination, capacities of both lines to store sperm in SSTs seems to be similar. This could be partly due to a similar molecular composition, including metabolites, that promotes sperm storage.

However, our study showed a clear separation between the F+ and the F- lines even at 24 hours, two weeks and three weeks after insemination, suggesting that the selection on reproductive performances has led to significant changes in the metabolomic profile of UF. Among the metabolites discriminant between the two lines, formate, lactate, myo-inositol, fumarate, succinate, dimethylamine and arabinose were the most preponderant.

Formate is the simplest carboxylic acid (HCOOH) involved in the particular at the crossroad between cellular and whole body metabolism. Its centrality confers formate with a key role in physiology (Pietzke et al., 2020). In mammals, formate is known to play a significant role in embryonic development. In folate-resistant mouse, formate supplementation rescued neural tube defects (Sudiwala et al., 2016; Kim et al., 2018). Moreover, our Metabolite Set Enrichment Analysis (MSEA) revealed an enrichment in steroid biosynthesis, and androgen, estrogen and androstenedione metabolisms, which all involved formate, suggesting this metabolite could play an important role in hormonal regulation, at least locally. It is of major importance considering that a local hormonal regulation after insemination has been described in turkey and hens (Long et al., 2003; Das, Nagasaka, et al., 2006; Foye-Jackson et al., 2011), and that estrogen play an essential role to maintain SST structures (Yoshimura et al., 2000). Considering that formate were significantly more abundant in F+ UF compared to F-, it could ensure the maintenance of SST structure and promotes long-term sperm storage in F+ hens.

Among the organic acids that were discriminant between the two lines, succinate and fumarate were significantly more abundant in F+ UF compared to F-. Succinate and fumarate are well known to be involved in acid citric cycle. Lactate was also significantly more abundant in F+ UF compared to F-. According to Matsuzaki et al. (2015), lactate accumulation in quails SST cells could participate to the regulation of resident sperm motility (Matsuzaki et al., 2015). These authors demonstrated that lactate at physiological concentration inhibits sperm motility *in vitro* by inducing sperm cytoplasmic acidification. Furthermore, they observed that others organic acid such as citrate and malate are also able to inhibit sperm motility (Matsuzaki et al., 2015). Several authors hypothesized a quiescent state of resident sperm in SSTs, with motility and metabolism being reversibly suppressed (Ashizawa et al., 1976; Bakst, 1985; Bakst & Bauchan, 2015; Matsuzaki et al., 2015). Considering our model of hens, higher lactate concentration in F+ UF could be a key factor to allow sperm to be quiescent in sperm reservoir, promoting a long-term sperm storage.

Moreover, our pathway impact analysis revealed an enrichment in pyruvate metabolism and citrate cycle (TCA) preponderant in F+ UF. Pyruvate is one of the most important product of the glycolysis. Pyruvate can be further metabolized to lactate that is the final product of aerobic glycolysis or transported into the mitochondria and converted to acetyl-CoA, which participates in the TCA cycle. Thus, the metabolization of pyruvate using glycolysis or TCA cycle may indicate whether cells use more glycolysis or oxidative phosphorylation, respectively. Considering that a majority of metabolites involved in TCA cycle and pyruvate metabolism are more abundant in F+ UF, these two pathways could be more activated in F+ reproductive tract than in F-.

Dimethylamine was significantly more abundant in the F+ UF than in the F- UF. Dimethylamine is an organic secondary amine. It is a colorless, liquefied and flammable gas. Dimethylamine have been identified in human seminal plasma and is positively correlated to the sperm motility (Engel et al., 2019).

Myo-inositol was a discriminant metabolite preponderant in the uterine fluid of F- hens in comparison with uterine fluid of F+ hens. The presence of myo-inositol has been previously demonstrated in the turkey uterovaginal junction and uterus (van der Horst & Litjens, 1969). The authors described the preservative role of myo-inositol for sperm motility *in vitro* (van der Horst & Litjens, 1969). In mammals, myo-inositol increased the sperm motility (Scarselli et al., 2016).

All along the time after insemination, the differences in UF metabolome between both lines exhibiting a short- (F-) and long-term (F+) sperm storage highlights the importance of several metabolites in the long-term sperm storage within SST. Therefore, the follow-up of UF metabolites before and until three weeks after insemination revealed that formate and lactate were constantly preponderant in F+ UF compared to F-UF (fold change: 1.10 to 1.65), suggesting that these metabolites are key factors all along the long-term sperm storage. In contrast, myo-inositol were constantly preponderant in F- UF (fold change: 0.80-0.94). Before insemination and during the first stage of sperm storage (24h after insemination), fumarate and succinate were more abundant in F+ UF compared to F- UF (fold change : 2.12 to 2.46), highlighting the importance of these metabolites at the establishment of the long-term sperm storage. During the late stage of sperm storage (two and three weeks after insemination), dimethylamine and arabinose were preponderant in F+ UF compared to F- UF (fold change: 2.02 to 3.34), suggesting that these metabolites could be essential at the late stage of long-term sperm storage.

Insemination effect

In this study, no significant SIMCA-models were found in F+ hens when we compared the effect of insemination after 24 hours, one week, two weeks and three weeks. Although the individual variability, this suggest that the composition of the UF metabolites in F+ hens is relatively stable after artificial insemination. In contrast in F- hens, we demonstrated that the composition of the UF metabolites was significantly modified after artificial insemination. F- line of hens can therefore be considered as a negative control for long-term sperm storage. Fumarate, dimethylamine, myo-inositol and formate were the most significantly modified. While fumarate increased progressively by approximatively threefold during the three weeks after insemination in F- UF, dimethylamine decreased progressively by approximatively threefold. Myo-inositol increased also during the three weeks after insemination (fold change: 1.11 to 1.34). Formate increased from the first week after insemination to the third week (fold change: 1.42 to 1.50). Despite its increase, formate amounts were constantly lower in F- UF compared to F+ UF, highlighting its importance for a long-term sperm storage in SSTs.

Our MSEA analysis revealed an enrichment in Warburg effect in F- UF. Warburg effect is well known as a modification of the common glycolysis pathway in cancer cells resulting in the high rates of glucose uptake and lactate secretion, even in aerobic condition (DeBerardinis & Chandel, 2020). In non-cancer cells, it have been shown that T lymphocytes induced a fast

445 glucose uptake when activated by CD28 pathway (Frauwirth et al., 2002). The majority of
446 glucose taken by CD28-activated T lymphocytes is metabolized to lactate and release out of the
447 cells (Frauwirth et al., 2002), suggesting that Warburg effect is a physiological phenomenon
448 that is not unique to cancer cells. Interestingly, it is admitted that insemination induces a local
449 immune regulation in hen's utero-vaginal junction, allowing sperm storage process (Das, Isobe,
450 et al., 2006; Atikuzzaman et al., 2017). A close association has been described between sperm
451 storage duration and uterovaginal expression of Transforming growth factor β (TGF-β), which
452 is a pleiotropic cytokine involved in both suppressive and inflammatory immune responses, and
453 TGF-β receptor (TβR) (Das et al.2006). The presence of TβR2 has been identified in the
454 uterovaginal lymphocytes, and it has been proposed that insemination induces an increase of
455 several TGFβs leading to the suppression of lymphocyte activation (Das, Isobe, et al., 2006).
456 In our study, Warburg effect involved several metabolites including glucose, fumarate and
457 lactate. We also found that Warburg effect pathway were enriched in genetic line effect (NS).
458 The metabolization of glucose in regards to immune regulation could be further investigated in
459 the context of sperm storage.

460 Amoung the metabolites that may have an influence on sperm motility, myo-inositol that
461 was constantly preponderant in F- UF compared to F+ UF, may support sperm motility (van
462 der Horst & Litjens, 1969; Scarselli et al., 2016). Moreover, although lactate amount increased
463 in F-UF after insemination (NS), it was constantly lower in F- UF compared to F+ UF. It is
464 possible that lactate quantity was not efficient in F- UF to promote sperm quiescence, which
465 can explain a short-term sperm storage (Matsuzaki et al., 2015). Moreover, protein acting as
466 sperm motility activator (HSPA8) has been already identified in higher quantity in the F- UF
467 (Riou et al., 2019) supporting evidence of molecules activator of sperm motility in the F- UF
468 that may explain the short-term sperm storage ability in F- hens. The high decrease of
469 dimethylamine in F- UF all along the period after insemination suggest that this metabolite can
470 be essential for long-term sperm storage. Its effect on fowl sperm functions needs to be further
471 investigated.

472 In conclusion, our study revealed that formate, dimethylamine, myo-inositol and organic
473 acids including lactate, succinate and fumarate, were discriminant between the UF from the two
474 genetic lines and represent key metabolites involved in sperm storage duration.

475 **References**

Ahammad, M. U., Miyazato, T., Nishino, C., Tatemoto, H., Okura, N., Okamoto, S., . . . Nakada, T. (2013). Effects of Fluid Secreted from the Uterus on Duration of Fertile Egg Production in Hens, and Survivability and Penetrability of Fowl Sperm in vitro. *Journal of Poultry Science, 50*(1), 74-82. doi:10.2141/jpsa.0120045

Ashizawa, K., Nishiyama, H., & Nagaen, T. (1976). Effets of oviducal cells on the survival and fertilizing ability of fowl spermatozoa. *J. Reprod. Fert., 47*, 305-311.

Atikuzzaman, M., Alvarez-Rodriguez, M., Vicente-Carrillo, A., Johnsson, M., Wright, D., & Rodriguez-Martinez, H. (2017). Conserved gene expression in sperm reservoirs between birds and mammals in response to mating. *BMC Genomics, 18*(1), 98. doi:10.1186/s12864-017-3488-x

Atikuzzaman, M., Mehta Bhai, R., Fogelholm, J., Wright, D., & Rodriguez-Martinez, H. (2015). Mating induces the expression of immune- and pH-regulatory genes in the utero-vaginal junction containing mucosal sperm-storage tubuli of hens. *Reproduction, 150*(6), 473-483. doi:10.1530/REP-15-0253

Bakst, M. R. (1985). Zinc reduces turkey sperm oxygen uptake in vitro. *Poult Sci, 64*(3), 564-566. Retrieved from http://www.ncbi.nlm.nih.gov/pubmed/3991430

Bakst, M. R., & Akuffo, V. (2007). Alkaline phosphatase reactivity in the vagina and uterovaginal junction sperm-storage tubules of turkeys in egg production: implications for sperm storage. *Br Poult Sci, 48*(4), 515-518. doi:10.1080/00071660701381761

Bakst, M. R., & Akuffo, V. (2009). Morphology of the turkey vagina with and without an egg mass in the uterus. *Poult Sci, 88*(3), 631-635. doi:10.3382/ps.2007-00527

Bakst, M. R., & Bauchan, G. (2015). Apical blebs on sperm storage tubule epithelial cell microvilli: their release and interaction with resident sperm in the turkey hen oviduct. *Theriogenology, 83*(9), 1438-1444. doi:10.1016/j.theriogenology.2015.01.016

Bakst, M. R., Wishart, G. J., & Brillard, J. P. (1994). Oviductal sperm selection, transport, and storage in poultry. *Poultry Science Reviews, 5*, 117-143.

Birkhead, T. R., & Moller, A. P. (1993). Sexual Selection and the Temporal Separation of Reproductive Events - Sperm Storage Data from Reptiles, Birds and Mammals. *Biological Journal of the Linnean Society, 50*(4), 295-311. doi:DOI 10.1111/j.1095-8312.1993.tb00933.x

Brillard, J. P. (1993). Sperm storage and transport following natural mating and artificial insemination. *Poult Sci, 72*(5), 923-928. Retrieved from http://www.ncbi.nlm.nih.gov/pubmed/8502613

Brillard, J. P., Beaumont, C., & Scheller, M. F. (1998). Physiological responses of hens divergently selected on the number of chicks obtained from a single insemination. *J Reprod Fertil, 114*(1), 111-117. Retrieved from http://www.ncbi.nlm.nih.gov/pubmed/9875162

Brillard, J. P., Galut, O., & Nys, Y. (1987). Possible causes of subfertility in hens following insemination near the time of oviposition. *Br Poult Sci, 28*(2), 307-318. doi:10.1080/00071668708416963

Das, S. C., Isobe, N., Nishibori, M., & Yoshimura, Y. (2006). Expression of transforming growth factor-beta isoforms and their receptors in utero-vaginal junction of hen oviduct in presence or absence of resident sperm with reference to sperm storage. *Reproduction, 132*(5), 781-790. doi:10.1530/rep.1.01177

Das, S. C., Isobe, N., & Yoshimura, Y. (2008). Mechanism of prolonged sperm storage and sperm survivability in hen oviduct: a review. *Am J Reprod Immunol, 60*(6), 477-481. doi:10.1111/j.1600-0897.2008.00651.x

Das, S. C., Nagasaka, N., & Yoshimura, Y. (2006). Changes in the expression of estrogen receptor mRNA in the utero-vaginal junction containing sperm storage tubules in

laying hens after repeated artificial insemination. *Theriogenology, 65*(4), 893-900. doi:10.1016/j.theriogenology.2005.07.004

DeBerardinis, R. J., & Chandel, N. S. (2020). We need to talk about the Warburg effect. *Nature Metabolism, 2*(2), 127-129. doi:10.1038/s42255-020-0172-2

Engel, K. M., Baumann, S., Rolle-Kampczyk, U., Schiller, J., von Bergen, M., & Grunewald, S. (2019). Metabolomic profiling reveals correlations between spermiogram parameters and the metabolites present in human spermatozoa and seminal plasma. *PLoS One, 14*(2), e0211679. doi:10.1371/journal.pone.0211679

Foye-Jackson, O. T., Long, J. A., Bakst, M. R., Blomberg, L. A., Akuffo, V. G., Silva, M. V., . . . McMurtry, J. P. (2011). Oviductal expression of avidin, avidin-related protein-2, and progesterone receptor in turkey hens in relation to sperm storage: effects of oviduct tissue type, sperm presence, and turkey line. *Poult Sci, 90*(7), 1539-1547. doi:10.3382/ps.2010-01159

Frauwirth, K. A., Riley, J. L., Harris, M. H., Parry, R. V., Rathmell, J. C., Plas, D. R., . . . Thompson, C. B. (2002). The CD28 Signaling Pathway Regulates Glucose Metabolism. *Immunity, 16*(6), 769-777. doi:https://doi.org/10.1016/S1074-7613(02)00323-0

Froman, D. (2003). Deduction of a model for sperm storage in the oviduct of the domestic fowl (Gallus domesticus). *Biol Reprod, 69*(1), 248-253. doi:10.1095/biolreprod.102.013482

Gautron, J., Guyot, N., Brionne, A., & Réhault-Godbert, S. (2019). CHAPTER 14 Bioactive Minor Egg Components. In *Eggs as Functional Foods and Nutraceuticals for Human Health* (pp. 259-284): The Royal Society of Chemistry.

Gautron, J., Hincke, M. T., & Nys, Y. (1997). Precursor matrix proteins in the uterine fluid change with stages of eggshell formation in hens. *Connect Tissue Res, 36*(3), 195-210. doi:10.3109/03008209709160220

Hincke, M. T., Gautron, J., Tsang, C. P., McKee, M. D., & Nys, Y. (1999). Molecular cloning and ultrastructural localization of the core protein of an eggshell matrix proteoglycan, ovocleidin-116. *J Biol Chem, 274*(46), 32915-32923. Retrieved from http://www.ncbi.nlm.nih.gov/pubmed/10551857

Kim, J., Lei, Y., Guo, J., Kim, S. E., Wlodarczyk, B. J., Cabrera, R. M., . . . Finnell, R. H. (2018). Formate rescues neural tube defects caused by mutations in Slc25a32. *Proc Natl Acad Sci U S A, 115*(18), 4690-4695. doi:10.1073/pnas.1800138115

Long, E. L., Sonstegard, T. S., Long, J. A., Van Tassell, C. P., & Zuelke, K. A. (2003). Serial analysis of gene expression in turkey sperm storage tubules in the presence and absence of resident sperm. *Biol Reprod, 69*(2), 469-474. doi:10.1095/biolreprod.102.015172

Marie, P., Labas, V., Brionne, A., Harichaux, G., Hennequet-Antier, C., Nys, Y., & Gautron, J. (2015). Quantitative proteomics and bioinformatics analysis provide new insight into protein function during avian eggshell biomineralization. *J Proteomics, 113*, 178-193.

Matsuzaki, M., Mizushima, S., Hiyama, G., Hirohashi, N., Shiba, K., Inaba, K., . . . Sasanami, T. (2015). Lactic acid is a sperm motility inactivation factor in the sperm storage tubules. *Sci Rep, 5*, 17643. doi:10.1038/srep17643

Pietzke, M., Meiser, J., & Vazquez, A. (2020). Formate metabolism in health and disease. *Molecular Metabolism, 33*, 23-37. doi:https://doi.org/10.1016/j.molmet.2019.05.012

Riou, C., Brionne, A., Cordeiro, L., Harichaux, G., Gargaros, A., Labas, V., . . . Gerard, N. (2019). Proteomic analysis of uterine fluid of fertile and subfertile hens before and after insemination. *Reproduction, 158*(4), 335-356. doi:10.1530/REP-19-0079

574 Riou, C., Brionne, A., Cordeiro, L., Harichaux, G., Gargaros, A., Labas, V., . . . Gerard, N.
575 (2020). Avian uterine fluid proteome: exosomes and biological processes potentially
576 involved in sperm survival. *Mol Reprod Dev, In Press*.
577 Riou, C., Cordeiro, L., & Gérard, N. (2017). Eggshell matrix proteins OC-116, OC-17 and
578 OCX36 in hen's sperm storage tubules. *Anim Reprod Sci., In press*.
579 Sasanami, T., Matsuzaki, M., Mizushima, S., & Hiyama, G. (2013). Sperm storage in the
580 female reproductive tract in birds. *J Reprod Dev, 59*(4), 334-338. Retrieved from
581 http://www.ncbi.nlm.nih.gov/pubmed/23965601
582 Scarselli, F., Lobascio, A. M., Terribile, M., Casciani, V., Greco, P., Franco, G., . . . Greco, E.
583 (2016). Analysis of MYO-Inositol effect on spermatozoa motility, in hyper viscous
584 ejaculates and in patients with grades II and III varicocele. *Arch Ital Urol Androl,*
585 *88*(4), 279-283. doi:10.4081/aiua.2016.4.279
586 Sudiwala, S., De Castro, S. C., Leung, K. Y., Brosnan, J. T., Brosnan, M. E., Mills, K., . . .
587 Greene, N. D. (2016). Formate supplementation enhances folate-dependent nucleotide
588 biosynthesis and prevents spina bifida in a mouse model of folic acid-resistant neural
589 tube defects. *Biochimie, 126*, 63-70. doi:10.1016/j.biochi.2016.02.010
590 Sun, C., Xu, G., & Yang, N. (2013). Differential label-free quantitative proteomic analysis of
591 avian eggshell matrix and uterine fluid proteins associated with eggshell mechanical
592 property. *Proteomics, 13*(23-24), 3523-3536. doi:10.1002/pmic.201300286
593 Tingari, M. D., & Lake, P. E. (1973). Ultrastructural studies on the uterovaginal sperm-host
594 glands of the domestic hen, Gallus domesticus. *J Reprod Fertil, 34*(3), 423-431.
595 Retrieved from http://www.ncbi.nlm.nih.gov/pubmed/4741313
596 van der Horst, C. J., & Litjens, J. B. (1969). Occurrence and determination of inositol in the
597 oviducts of turkey and hen. *Nature, 221*(5175), 86-87. doi:10.1038/221086a0
598 van Tienhoven, A. (1960). The metabolism of fowl sperm in different diluents. *The Journal of*
599 *Agricultural Science, 54*(1), 67-80. doi:10.1017/S002185960002147X
600 Yoshimura, Y., Koike, K., & Okamoto, T. (2000). Immunolocalization of progesterone and
601 estrogen receptors in the sperm storage tubules of laying and diethylstilbestrol-injected
602 immature hens. *Poult Sci, 79*(1), 94-98. Retrieved from
603 http://www.ncbi.nlm.nih.gov/pubmed/10685895

604

605

606 **Figure legends**

607 Figure 1. histogramme

608 Figure 2 : spectre légendé

609 Figure 3. Metabolites content of UF collected from virginized F+ hens. (A) Proportion of UF
610 metabolites (%) classified in super classes. Two super classes are detailed in sub classes. The
611 lists of metabolites that composed the sub classes are illustrated. (B) Concentration (%) of the
612 metabolites identified in UF.

613 Figure 4. Comparison between F+ and F- ^{1}H-NMR spectral data. (A) Model characteristics
614 R2Y and Q of the F+ vs F- genetic effect. AI: artificial insemination. (B) Score plot of the
615 model following OPLS-DA, resulted in 1 predictive and 1 orthogonal component (1p + 1o)
616 with the predictive ability *Q2*(cum) = 0.44 and the overall proportion of the variation in Y
617 explained by the model *R2Y(cum)* = 0.69. (C) Boxplot of formic and succinic acid
618 concentrations in both genetic lines (*: $p<0.05$).

619 Figure 5. Boxplots of formic acid, D-arabinose, D-lactic acid, myo-inositol, dimethylamine,
620 fumaric acid concentration in each lines at each time of collection (*: $p<0.05$). 1, virginized; 2,
621 24 hours after insemination; 3, one week after insemination; 4, two weeks after insemination;
622 5, three weeks after insemination. F+ in purple, F- in pink.

623 Figure 6. Comparisons between virginized and inseminated F- hens. (A) Model characteristics
624 R2Y and Q of the insemination effect. AI: artificial insemination. (B) Boxplots of
625 dimethylamine, formic acid, fumaric acid and myo-inositol concentration at each time of
626 collection (*: $p<0.05$). 1, virginized; 2, 24 hours after insemination; 3, one week after
627 insemination; 4, two weeks after insemination; 5, three weeks after insemination.

628 Figure 7. Summary of pathway impact analysis (A) and metabolic set enrichment analysis
629 (MSEA) (B) of the discriminating metabolites involved in genetic effect. (A) Graphic
630 representation of the impact of pathway involving discriminant metabolites (*p-value <0.05).
631 The x-axis represents the pathway impact, and the y-axis represents the log (p-value). (B) Bar
632 chart of the metabolite sets enrichments. The used metabolite entities were Formic acid,
633 Succinic acid, Fumaric acid, Lactic acid, Glucose, Arabinose, Dimethylamine, Alanine, myo-
634 Inositol, Mannose, Pyruvate and Citric acid. The most significant p-values are in red ($p<0.05$)
635 while the least significant are in yellow and white.

Figure 8. Summary of pathway impact analysis (A) and metabolic set enrichment analysis (MSEA) (B) performed using discriminating metabolites involved in insemination effect in F-UF. (A) Graphic representation of the impact of pathway involving discriminant metabolites (*p-value <0.05). The x-axis represents the pathway impact, and the y-axis represents the log (p-value). (B) Bar chart of the metabolite sets enrichments. The used metabolite entities were Glucose, Mannose, Arabinose, Lactic acid, Creatinine, Citric acid, Acetic acid, Succinic acid, Pyruvic acid, Glucuronic acid, Alanine, Dimethylamine, Formic acid, Fumaric acid, and myo-Inositol. The most significant p-values are in red ($p<0.05$) while the least significant are in yellow and white.

646 **Table 1**. Fertility traits

647

648

649 **Table 2**. Metabolites discrimining the two lines of hens. The uterine fluid metabolomic
650 composition from F+ hens was compared to the ones of F- hens, at each conditions, i.e.
651 virginized, 24 hours, 1 week, 2 weeks or 3 weeks after insemination.

Metabolites	*VIP*[a]	*FC*[b]	*P-value*[c]
Virginized			
Formate	1.52	**1.43**	0.040
Succinate	1.14	**2.46**	0.049
Myo-inositol	1.04	0.80	0.189
Fumaric acid	0.97	**2.19**	0.093
Lactic acid	0.74	**1.47**	0.232
Glucose	0.59	**1.01**	0.336
Inseminated, 24 hours after			
Formate	1.75	**1.65**	0.001
Lactic acid	1.20	**1.56**	0.0426
Fumaric acid	1.10	**2.12**	0.228
Glucose	0.98	0.98	0.181
Myo-inositol	0.95	0.94	0.490
Mannose	0.73	0.73	0.755
Inseminated, 2 weeks after			
Arabinose	1.36	**2.36**	0.035
Dimethylamine	1.34	**3.34**	0.014
Formate	1.33	**1.38**	0.051
Unidentified 3.15	1.11	**2.22**	0.138
Myo-inositol	0.95	0.80	0.073
Citrate	0.89	0.79	0.234
Fumaric acid	0.88	0.55	0.180
Lactic acid	0.81	**1.29**	0.295
Glucose	0.74	0.97	0.366
Alanine	0.73	**1.29**	0.445
Inseminated, 3 weeks after			
Myo-inositol	1.27	0.82	0.073
Formate	1.00	**1.32**	0.149
Pyruvate	0.99	**1.62**	0.268
Unidentified 3.15	0.96	**2.19**	0.149
Dimethylamine	0.91	**2.02**	0.202
Lactic acid	0.24	**1.10**	0.756

652 [a]VIP = Variable Importance in Projection in the OPLS-DA model.
653 [b]FC = Fold-change ratio (F+/F-). The more highly concentrated metabolites in F+ than in F-
654 line are indicated in bold. [c]Welch's means equality t-test at 95% confidence level.

655 **Table 3**. Metabolites discrimining the effect of insemination at different period of sperm storage
656 in F- hens. The uterine fluid from virginized hens was compared to the uterine fluid from
657 inseminated hens, at 24 hours, 1 week, 2 weeks or 3 weeks after insemination.

Metabolites	*VIP*[a]	*FC*[b]	*P-value*[c]
Virginized vs Inseminated, 24 hours after			
Fumaric acid	1.69	**2.19**	0.028
Dimethylamine	1.25	0.59	0.105
Myo-inositol	0.75	**1.11**	0.279
Glucuronate	0.72	**1.17**	0.195
Arabinose	0.71	0.76	0.574
Glucose	0.04	0.99	0.960
Virginized vs Inseminated, 1 week after			
Formate	1.38	**1.50**	0.021
Myo-inositol	1.17	**1.37**	0.059
Dimethylamine	1.17	0.46	0.046
Fumaric acid	1.17	**2.46**	0.112
Lactic acid	1.02	**1.63**	0.093
Unidentified 3.15	0.98	0.47	0.236
Glucose	0.87	**1.02**	0.114
Arabinose	0.80	0.74	0.312
Virginized vs Inseminated, 2 weeks after			
Fumaric acid	1.38	**2.98**	0.015
Myo-inositol	1.18	**1.34**	0.021
Formate	1.13	**1.42**	0.094
Dimethylamine	1.13	0.44	0.029
Lactic acid	1.06	**1.63**	0.121
Arabinose	0.95	0.56	0.121
Unidentified 3,15	0.77	0.51	0.613
Mannose	0.65	0.89	0.336
PPG	0.62	0.84	0.534
Virginized vs Inseminated, 3 weeks after			
Fumaric acid	1.31	**3.45**	0.040
Dimethylamine	1.24	0.34	0.014
Myo-inositol	1.18	**1.34**	0.014
Formate	0.96	**1.45**	0.094
Glucuronate	0.90	**1.53**	0.189
Glucose	0.81	**1.02**	0.281
Lactic acid	0.81	**1.59**	0.189

658 [a]VIP = Variable Importance in Projection in the OPLS-DA model.
659 [b]FC = Fold-change ratio (after insemination/ virginized). The more highly concentrated
660 metabolites in inseminated hens than in virginized hens are indicated in bold.
661 [c]Welch's means equality t-test at 95% confidence level.
662

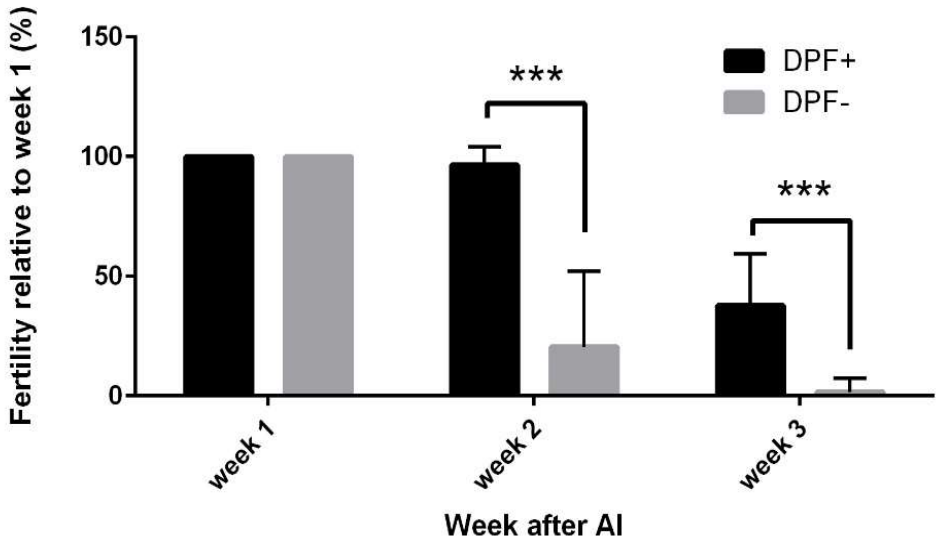

663
664 Figure 1
665

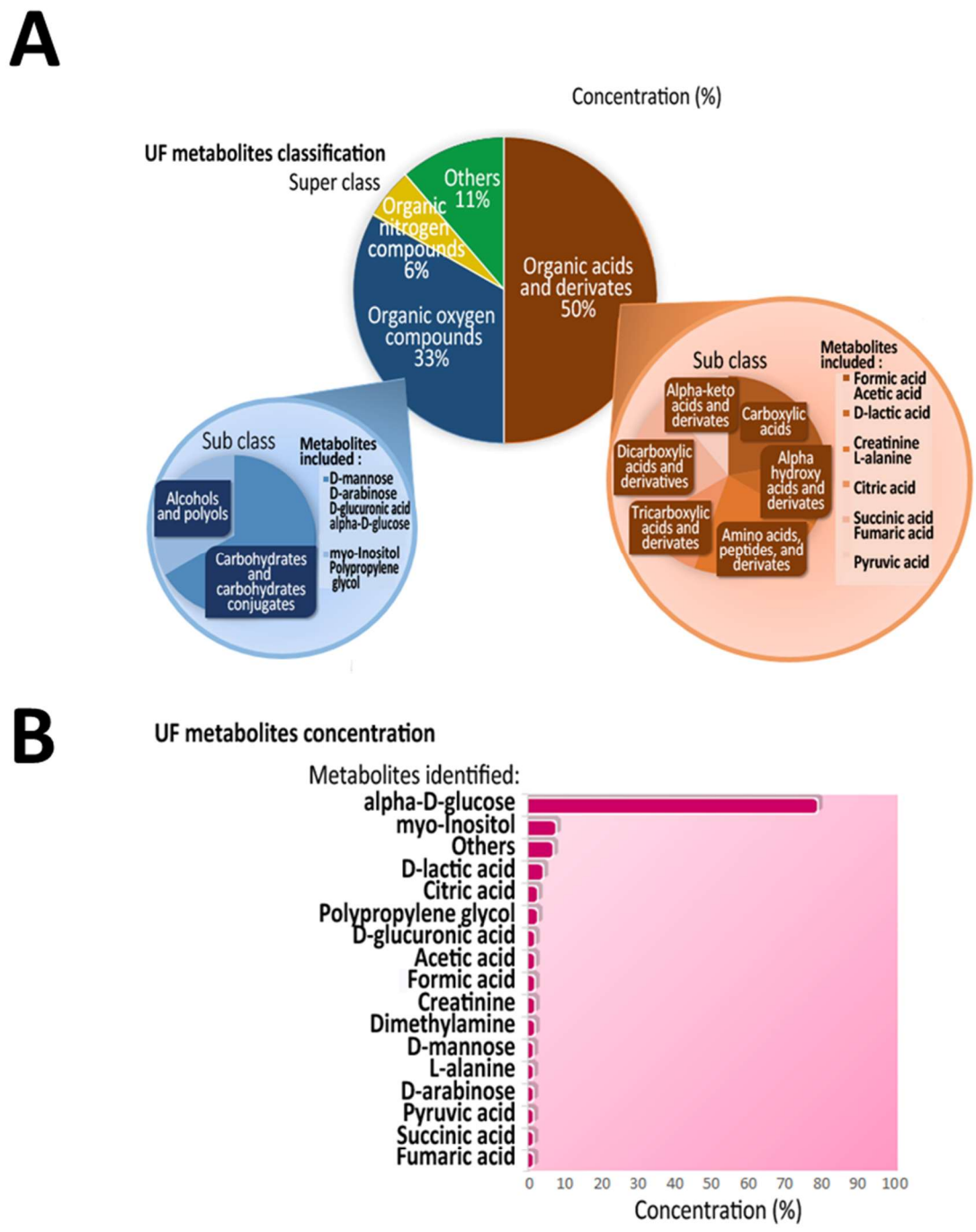
A
Concentration (%)
UF metabolites classification
Super class
Others 11%
Organic nitrogen compounds 6%
Organic oxygen compounds 33%
Organic acids and derivates 50%
Sub class
Metabolites included :
Alcohols and polyols
Carbohydrates and carbohydrates conjugates
D-mannose
D-arabinose
D-glucuronic acid
alpha-D-glucose
myo-Inositol
Polypropylene glycol
Sub class
Metabolites included :
Alpha-keto acids and derivates
Carboxylic acids
Dicarboxylic acids and derivatives
Alpha hydroxy acids and derivates
Tricarboxylic acids and derivates
Amino acids, peptides, and derivates
Formic acid
Acetic acid
D-lactic acid
Creatinine
L-alanine
Citric acid
Succinic acid
Fumaric acid
Pyruvic acid
B
UF metabolites concentration
Metabolites identified:
alpha-D-glucose
myo-Inositol
Others
D-lactic acid
Citric acid
Polypropylene glycol
D-glucuronic acid
Acetic acid
Formic acid
Creatinine
Dimethylamine
D-mannose
L-alanine
D-arabinose
Pyruvic acid
Succinic acid
Fumaric acid
0 10 20 30 40 50 60 70 80 90 100
Concentration (%)

Figure 3

A

Model characteristics, R2Y and Q	*R2Y*	*Q2*
Virginized	0.69	0.44
Inseminated, 24h after AI	0.66	0.44
Inseminated, 2 weeks after AI	0.76	0.52
Inseminated, 3 weeks after AI	0.75	0.38

B

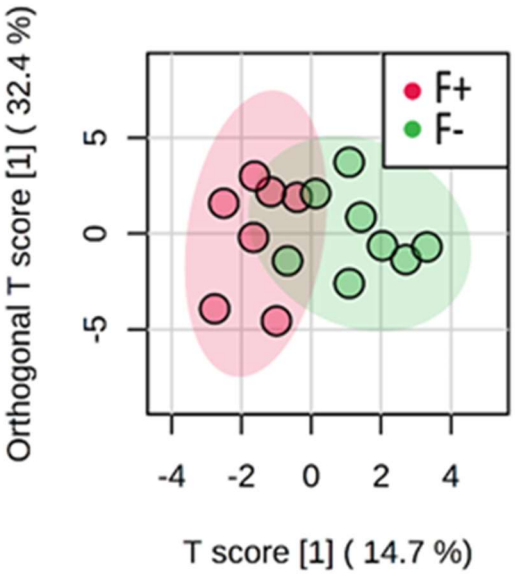

C

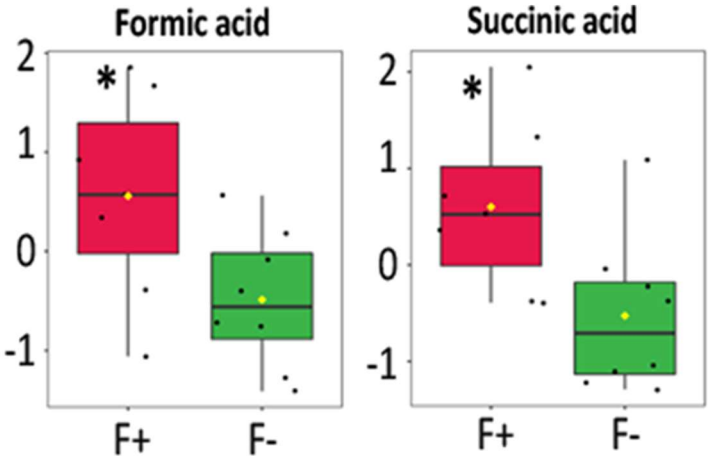

Figure 4

672
673

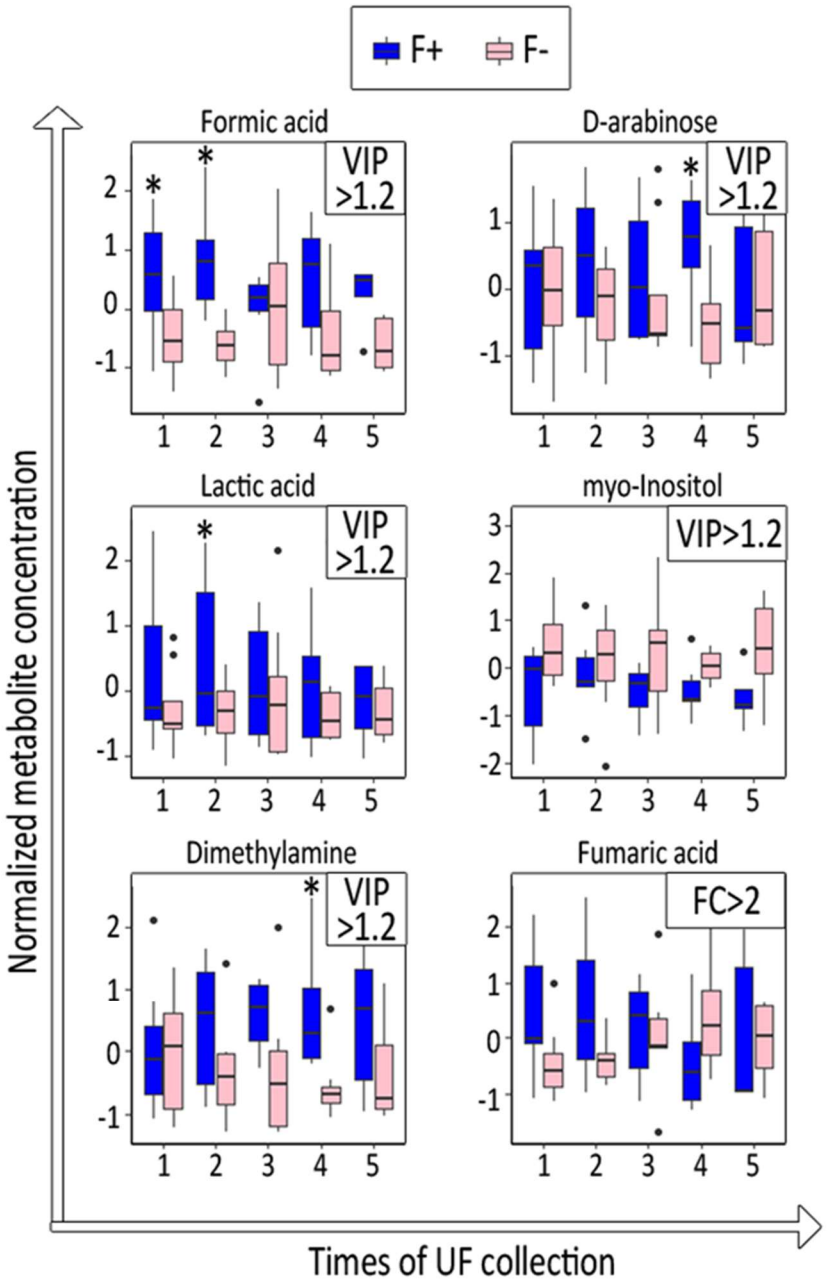

Figure 5

674
675

A

Model characteristics, R2Y and Q	***R2Y***	***Q2***
Virginized vs inseminated 24h after AI	0.66	0.27
Virginized vs inseminated 1 week after AI	0.60	0.36
Virginized vs inseminated 2 week after AI	0.63	0.45
Virginized vs inseminated 3 week after AI	0.72	0.50

B

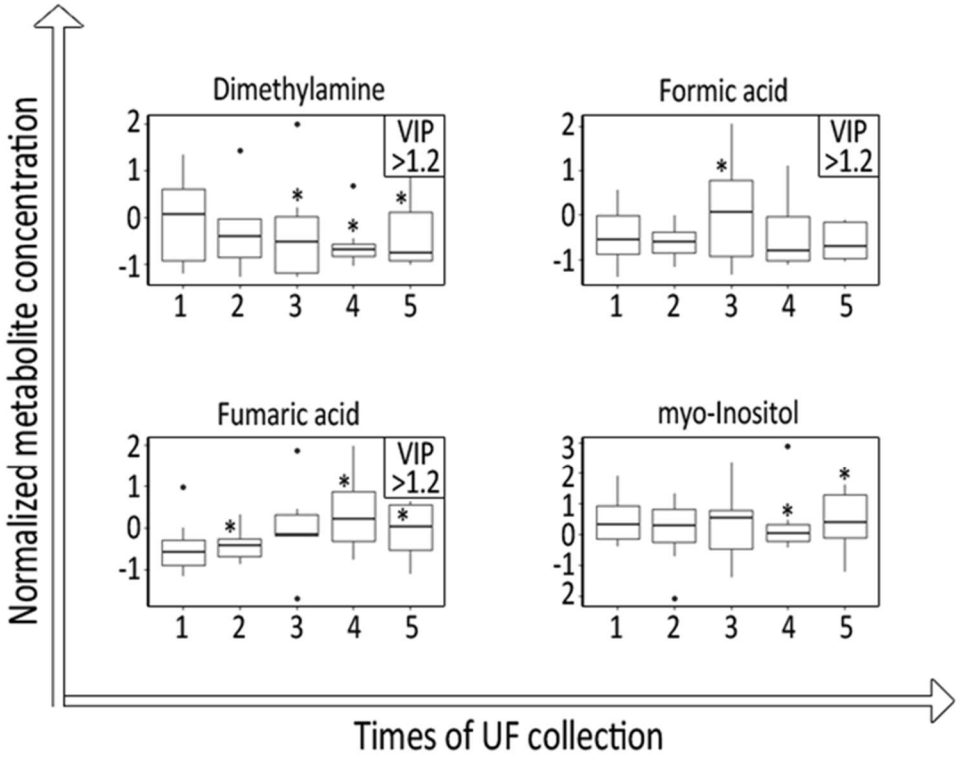

Figure 6

676
677

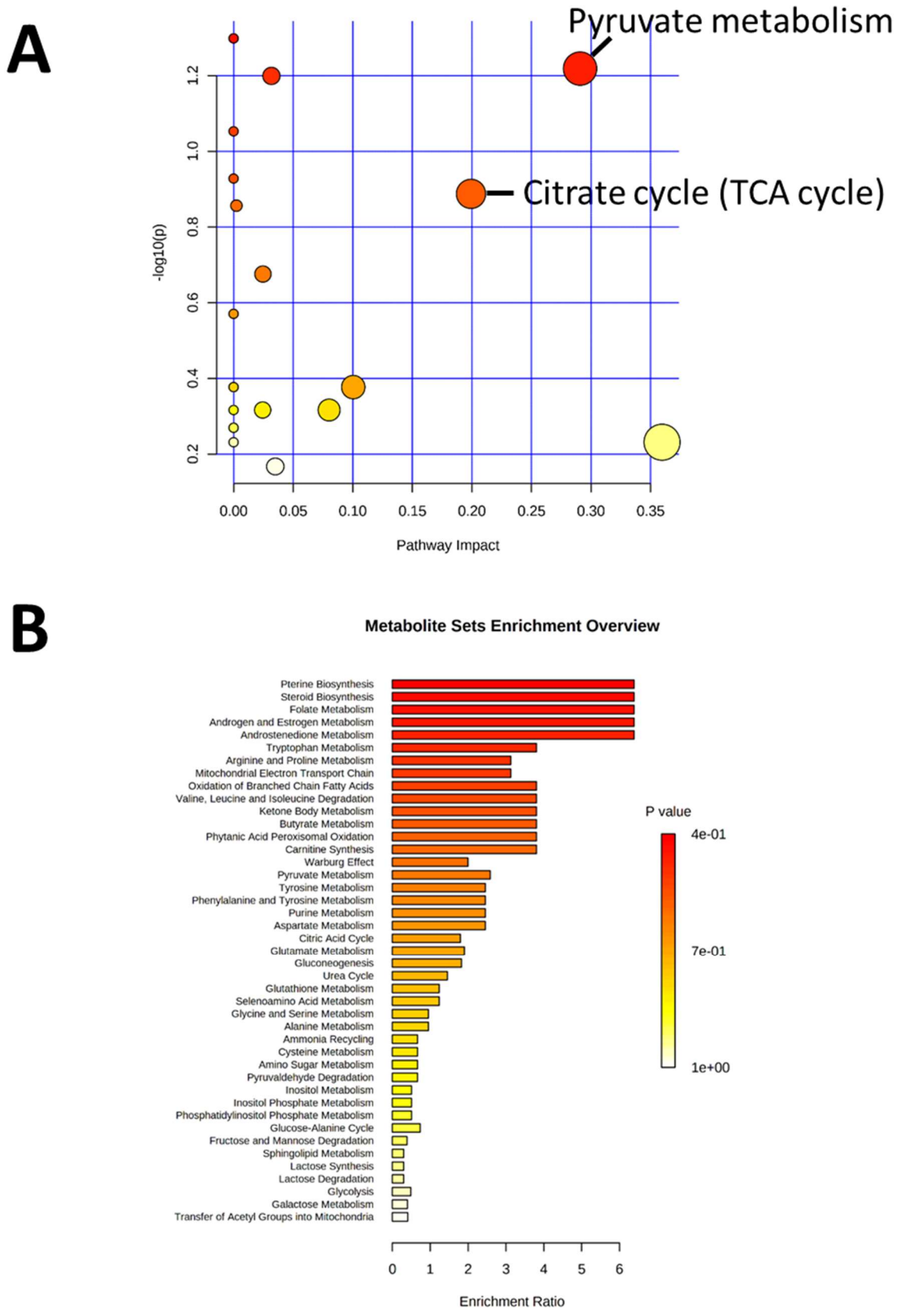
A
Pyruvate metabolism
Citrate cycle (TCA cycle)
-log10(p)
0.2
0.4
0.6
0.8
1.0
1.2
0.00
0.05
0.10
0.15
0.20
0.25
0.30
0.35
Pathway Impact
B
Metabolite Sets Enrichment Overview
Pterine Biosynthesis
Steroid Biosynthesis
Folate Metabolism
Androgen and Estrogen Metabolism
Androstenedione Metabolism
Tryptophan Metabolism
Arginine and Proline Metabolism
Mitochondrial Electron Transport Chain
Oxidation of Branched Chain Fatty Acids
Valine, Leucine and Isoleucine Degradation
Ketone Body Metabolism
Butyrate Metabolism
Phytanic Acid Peroxisomal Oxidation
Carnitine Synthesis
Warburg Effect
Pyruvate Metabolism
Tyrosine Metabolism
Phenylalanine and Tyrosine Metabolism
Purine Metabolism
Aspartate Metabolism
Citric Acid Cycle
Glutamate Metabolism
Gluconeogenesis
Urea Cycle
Glutathione Metabolism
Selenoamino Acid Metabolism
Glycine and Serine Metabolism
Alanine Metabolism
Ammonia Recycling
Cysteine Metabolism
Amino Sugar Metabolism
Pyruvaldehyde Degradation
Inositol Metabolism
Inositol Phosphate Metabolism
Phosphatidylinositol Phosphate Metabolism
Glucose-Alanine Cycle
Fructose and Mannose Degradation
Sphingolipid Metabolism
Lactose Synthesis
Lactose Degradation
Glycolysis
Galactose Metabolism
Transfer of Acetyl Groups into Mitochondria
P value
4e-01
7e-01
1e+00
0
1
2
3
4
5
6
Enrichment Ratio

Figure 7

678

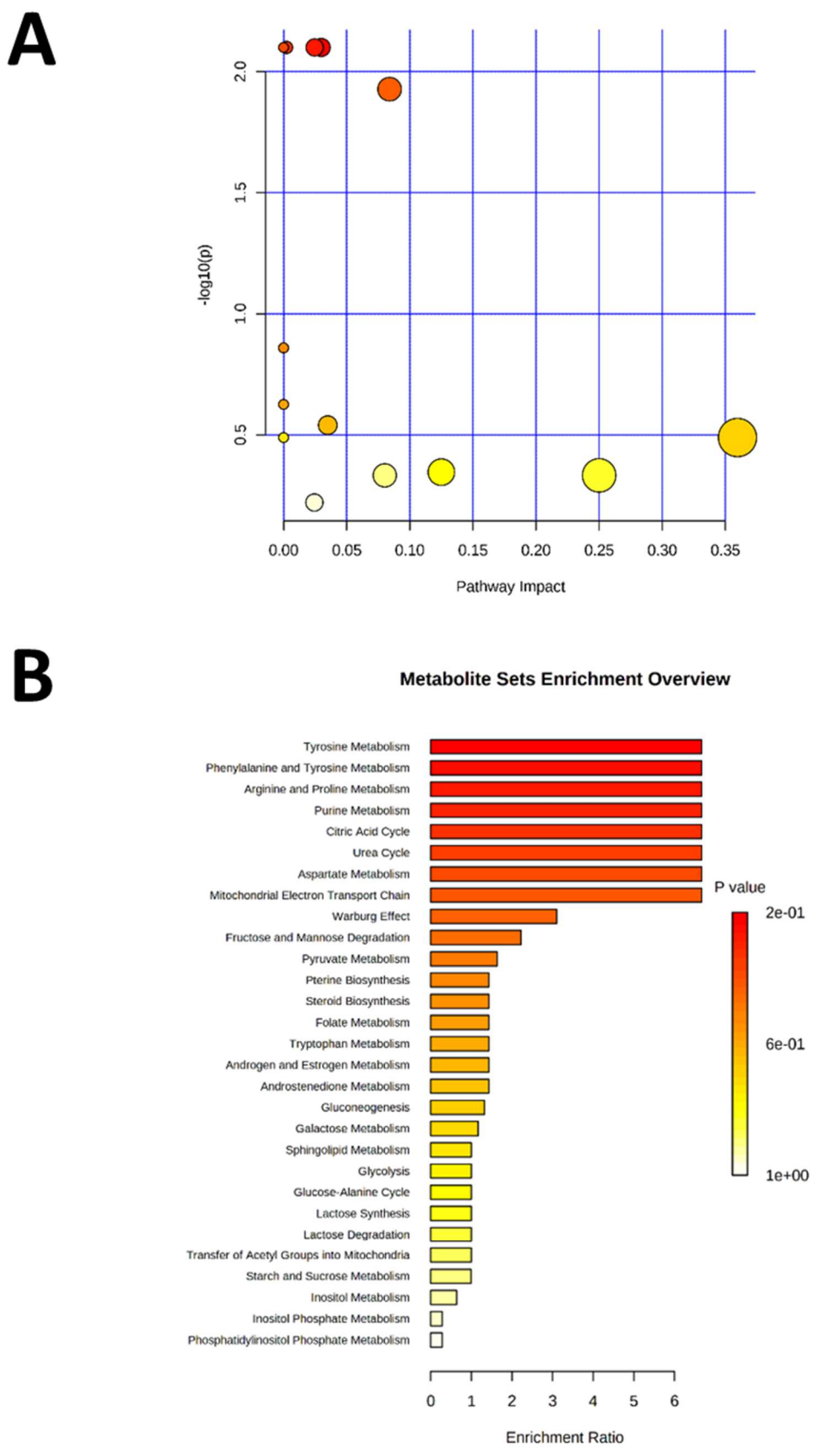
A
-log10(p)
2.0
1.5
1.0
0.5
0.00
0.05
0.10
0.15
0.20
0.25
0.30
0.35
Pathway Impact
B
Metabolite Sets Enrichment Overview
Tyrosine Metabolism
Phenylalanine and Tyrosine Metabolism
Arginine and Proline Metabolism
Purine Metabolism
Citric Acid Cycle
Urea Cycle
Aspartate Metabolism
Mitochondrial Electron Transport Chain
Warburg Effect
Fructose and Mannose Degradation
Pyruvate Metabolism
Pterine Biosynthesis
Steroid Biosynthesis
Folate Metabolism
Tryptophan Metabolism
Androgen and Estrogen Metabolism
Androstenedione Metabolism
Gluconeogenesis
Galactose Metabolism
Sphingolipid Metabolism
Glycolysis
Glucose-Alanine Cycle
Lactose Synthesis
Lactose Degradation
Transfer of Acetyl Groups into Mitochondria
Starch and Sucrose Metabolism
Inositol Metabolism
Inositol Phosphate Metabolism
Phosphatidylinositol Phosphate Metabolism
P value
2e-01
6e-01
1e+00
0
1
2
3
4
5
6
Enrichment Ratio

Figure 8

679